Supporting Information : Insights into the $\pi-\pi$ interaction driven non-covalent functionalization of carbon nanotubes of various diameters by conjugated fluorene and carbazole copolymers

Robert Benda,[1,2,a] Gaël Zucchi,[1] Eric Cancès,[2] and Bérengère Lebental[1,3]
[1)]*LPICM, CNRS, Ecole Polytechnique, Institut Polytechnique de Paris, Route De Saclay, 91128 Palaiseau, France*
[2)]*CERMICS, Ecole des Ponts and INRIA, Université Paris-Est, 6-8 avenue Blaise Pascal 77455 Marne-la-Vallée, France*
[3)]*Université Paris-Est, IFSTTAR, 14-20, Boulevard Newton, 77420 Champs-sur-Marne, France*

In this supporting information, we validate our use of ReaxFF force field to perform simulations of CNT/polymer compounds. A benchmark and comparison of ReaxFF results with higher levels of theory is done, for the adsorption geometries and binding energies in typical $\pi-\pi$ interacting compounds of polycyclic aromatic hydrocarbons on top of a graphene sheet.

A. Introduction

Our use of ReaxFF force field (with the parametrization for elements C, H, O and N taken from Ref.[1]) to study the geometry of conjugated polymers adsorbed non-covalently on CNT (*i.e.* graphene like) surfaces has to be validated. We thus performed a benchmark for binding energies and adsorption geometries of small organic molecules on graphene – at different equilibrium positions of these molecules on the sheet, which can be deemed as 'adsorption modes' (following the idea of Refs.[2,3] In particular, the difference in energy between the 'ABAB' stacking geometry (see *e.g.* figure 2) and the 'AAAA' sandwich (or 'hollow') geometry (see *e.g.* figure 1) is discussed in all cases. From the corresponding results, we will justify our choice of overlooking the dependence on the nanotube chirality in the previously described simulation results. Indeed, large diameter (of low curvature) carbon nanotubes are locally well approximated by a graphene sheet.

The physisorption of benzene (6 carbon atoms), perylene (20 carbon atoms, five benzene cycles – four only being aromatic), and a 'large coronene' molecule (378 carbon atoms, locally approximating a graphene sheet) are studied. The model surface is a graphene sheet hydrogenated at the edges, made up of 956 atoms (including the hydrogen atoms at the edges of the sheet) for the case of benzene and perylene, and of 13,772 atoms for the 'large coronene' molecule. The size of this graphene sheet is chosen large enough so that the initial relaxation ripples of the sheet upon minimization (appearing for instance when an organic molecule is initially very close to the sheet, which yields initial high forces) vanish over a characteristic distance much smaller than the sheet dimension. No periodic boundary conditions are used in the following structural minimizations, so that the aromatic molecules only interact with the sheet underneath, and not with their replicas (which would be periodically repeated in space in the case of periodic boundary conditions).

B. Methodology

Both the organic molecule and the graphene sheet are allowed to relax during structural minimizations. Benzene is placed initially on top of graphene at different adsorption sites, following the six main adsorption sites described by Kozlov *et al.*[4] 'Sandwich' (hollow) configurations refer to the adsorption sites being located right above hexagons of graphene (*AA* stacking) while 'stacked' configurations refer to the *ABAB* stacking (Bernal stacking) which is found in graphite – *i.e.* half of the molecule carbon atoms being on top of hexagon centers of the layer underneath, the other half being exactly on top of another carbon atom.

The total adsorption energy should arguably be roughly additive with the number of carbon atoms in the adsorbed aromatic molecule. We thus performed similar minimizations for bigger aromatic molecules, generalizing benzene (perylene, 'large coronene'). Two top views of initial 'sandwich' (AA) and 'stacked' (AB) geometries for the perylene molecule are displayed in figures 1 and 2. The 'large coronene' molecule (made up of 426 atoms, including 378 carbon atoms) is located initially

[a)]Electronic mail: robert.benda@polytechnique.org

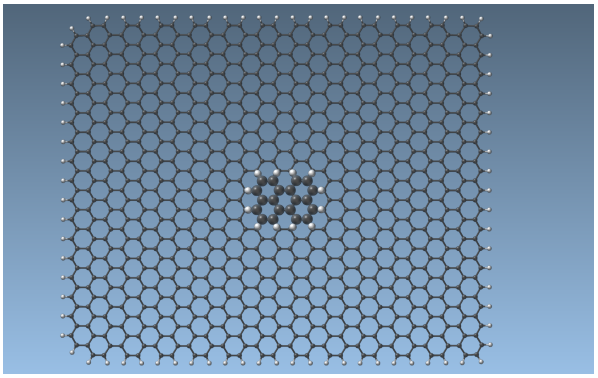

FIG. 1: 'Sandwich' adsorption site studied for perylene on a model graphene sheet (hydrogenated at the edges to avoid unsaturated effects)

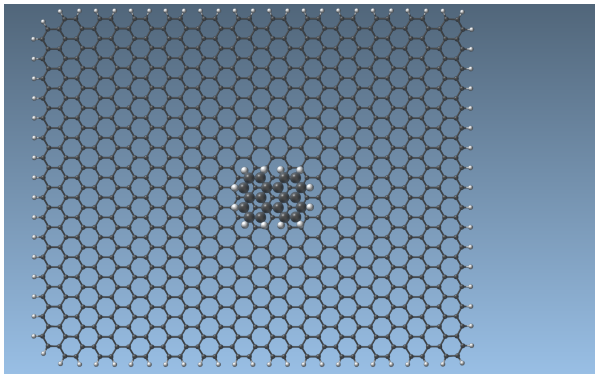

FIG. 2: 'Stacked' adsorption site studied for perylene on a model graphene sheet (hydrogenated at the edges to avoid unsaturated effects)

on top of a much larger graphene sheet than for benzene and perylene, to avoid any egde effect (see figures 3 and 4). For this large molecule we also minimize an initially 'incommensurate' geometry, where the molecule is rotated with respect to the underlying graphene surface from the stacked *AB* geometry. We want the size of the aromatic molecule to be much smaller than the dimension of the graphene sheet underneath, so that only $\pi - \pi$ interactions occur and no possible edge or curvature effects, due to finite-size effects, can take place. Therefore we chose a square graphene sheet of 20 nm per 20 nm (hydrogenated at the edges to avoid carbon unsaturated effects), made up of 13,772 atoms, to probe the interaction of the 'large coronene' molecule with graphene. Let us point out that the adsorption of 'large coronene' on graphene mimicks a system made up of two graphene sheets, in particular around the molecule center. Besides, it is known that the density of states and electronic structure of large polycyclic aromatic molecules converge quickly to those of graphene with increasing size.[5] This choice of large molecule, similar to a graphene monolayer, thus allows to compare to literature calculations on bilayer graphene.

C. Results

Benzene :

At the end of the minimization, benzene always remains perfectly parallel to the sheet (for all adsorption sites), the graphene sheet being almost planar. The sheet displays very light corrugations of about 0.2 $\AA$ (as a maximum), also reported in the DFT-D study[4] (from 4 to 13 pm corrugation depending on the coverage of the graphene sheet by adsorbed molecule). **In this study,[4] all systems were periodized, so that plane wave basis sets were used (cutoff energy 415 eV, Projector Augmented Wave method), in conjunction with the PBE functional (GGA type) and semi-empirical dispersion corrections.**[6]

ReaxFF is found to slightly overestimate adsorption energies for $\pi - \pi$ interactions of benzene on graphene, around 2.7 kcal/mol (*i.e.* 114 meV) per carbon atom of benzene (see Table I). Indeed, experimental thermal desorption spectroscopy measurements for aromatic molecules (benzene, naphtalene, coronene $C_{24}H_{12}$, ovalene) on graphite lead to a binding energy (identified to activation energy for desorption) per carbon atom of the aromatic molecule being 52 $\pm$ 5 meV[7] – average over the different aromatic molecules of varying sizes studied. Yet, DFT-D calculations in Ref.[4] yielded from 2.6 to 3.1 kcal/mol (*i.e.* 114 to 135 meV) interaction energy per carbon atom , a range of values close to that derived with ReaxFF.

The adsorption energy of benzene on graphene computed here with ReaxFF in the stacked geometry (707 meV, see below) can also be compared with the results of Ershova and al. in[8] who found about 470 meV total binding energy at the ωB97X-D/6-31G* level of theory[9] (hybrid functional with long-range Coulomb-attenuation and Grimme semi-empirical corrections for dispersion interactions[10] – damped pairwise interactions terms – and using 6-31G* basis set). This DFT functional is one of the best performing energy model on the S22 benchmark set[11] for weakly interacting complexes (see the review Ref.[12]).

The van der Waals (dispersion) contribution is found to dominate adsorption energies in all adsorption modes (for benzene, and also for the larger aromatic molecules studied), and appears as the main driving force. This will be

Benzene adsorption geometry	Adsorption energy (ReaxFF)	Adsorption energy ([4])	Adsorption distance (ReaxFF)	Adsorption distance ([4])
Stacked	-16.25	-18.83	3.22	3.22
Sandwich	-16.10	-17.69	3.23	3.26
'pd1'	-16.24	-18.62	3.20	3.22
'pd2'	-16.23	-18.36	3.23	3.18
'rst'	-16.20	-18.69	3.22	3.22
'rsw'	-16.22	-17.78	3.22	3.23

TABLE I: Comparison of adsorption energies of benzene (C_6H_6) on a graphene sheet (for the different adsorption sites proposed in Ref.,[4] whose labels 'pd1', 'pd2' – parallely displaced geometries –, 'rst' – rotated stacked –, 'rsw' – rotated sandwich – have been kept) computed with ReaxFF and with DFT-D (PBE exchange-correlation functional (GGA type), semi-empirical corrections[6] to account for vdW interactions, plane-wave basis set).[4] Energies are expressed in kcal/mol and distances in $\mathring{A}$.

further discussed in the concluding analysis and – in the point of view of its contribution to the AB/AA energy barrier – in the summarizing tables V, VI and VII.
The relative stability order of all the possible adsorption sites of benzene on graphene shows discrepancies between DFT-D[4] and ReaxFF (see classifications 1 and 2). Indeed, the relative stability order of the different adsorption geometries (proposed in Ref.,[4] whose labels have been kept) found with ReaxFF is the following (see table I) :

$$E_{Stacked} < E_{pd1} < E_{pd2} < E_{rsw} < E_{rst} < E_{sandwich} \quad (1)$$

to be compared to the relative stability order of the different adsorption geometries found with DFT-D,[4] from table I :

$$E_{Stacked} < E_{rst} < E_{pd1} < E_{pd2} < E_{rsw} < E_{sandwich} \quad (2)$$

Moreover, the order of magnitude of the adsorption energy difference between the two extreme stacked and sandwich configurations is much lower with ReaxFF in comparison to DFT-D results. With ReaxFF, the difference of adsorption energy between the stacked and sandwich configuration is (see table I) :

$$\Delta E^{ReaxFF}_{Stacked/Sandwich} = -0.15 \text{ kcal/mol} \approx -6.5 \text{ meV} \quad (3)$$

This difference of adsorption energy corresponds to 1.1 meV per carbon atom of benzene. From DFT-D (method of Ref.[4]), the difference of adsorption energy between the stacked and sandwich configuration is in turn (see table I) :

$$\Delta E^{DFT}_{Stacked/Sandwich} = -1.1 \text{ kcal/mol} \approx -49 \text{ meV} \quad (4)$$

i.e. a difference of energy of 8.2 meV per carbon atom between the stacked and sandwich configurations, about 7 times higher than the difference found by ReaxFF. These two adsorption modes are therefore much more separated in energy by the DFT-D[4] total energy than the ReaxFF force field.

Perylene :

The adsorption energy found with ReaxFF for a perylene molecule on top of a graphene sheet is about 2.2 kcal/mol (*i.e.* 97 meV) per carbon atom, to be compared with the 2.7 kcal/mol (*i.e.* 114 meV) per carbon atom found for a benzene molecule on top of graphene. The magnitude of this adsorption energy compares well with that of DFT-D[4] calculations. Again, the stacked configuration is more stable than the sandwich configuration with ReaxFF, the difference of adsorption energies between the stacked and sandwich configurations with ReaxFF being (see table II) :

$$\Delta E^{ReaxFF}_{Stacked/Sandwich} = -0.46 \text{ kcal/mol} \approx -20 \text{ meV} \quad (5)$$

This difference of adsorption energies is of 1.0 meV per carbon atom (20 carbon atoms in perylene). The difference of adsorption energies between the stacked and sandwich configurations of perylene on top of graphene, computed with DFT-D (method of Ref.[4]) (see table II) is in turn :

$$\Delta E^{DFT}_{Stacked/Sandwich} = -3.7 \text{ kcal/mol} \approx -156 \text{ meV} \quad (6)$$

i.e. of order 7.8 meV/C atom. Again, the two adsorption modes ('stacked' and 'sandwich') are therefore much more separated in energy by the DFT-D calculation[4] than the ReaxFF calculation.

Perylene adsorption geometry	Adsorption energy (ReaxFF)	Adsorption energy ([4])	Adsorption distance (ReaxFF)	Adsorption distance ([4])
Stacked	-44.75	-52.46	3.27	3.21
Sandwich	-44.29	-48.73	3.28	3.31

TABLE II: Comparison of adsorption energies of perylene (20 carbon atoms) on a graphene sheet computed with ReaxFF and with DFT-D (PBE exchange-correlation functional (GGA type), semi-empirical corrections[6] to account for vdW interactions, plane-wave basis set).[4] Energies are expressed in kcal/mol and distances in $\mathring{A}$

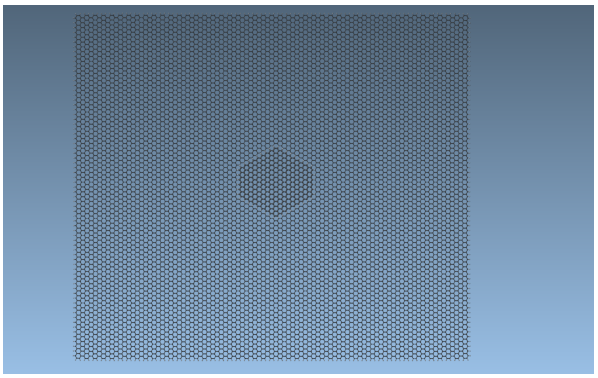

FIG. 3: 'Sandwich' adsorption site studied for the 'large coronene' molecule on a large (20 nm per 20 nm) model graphene sheet (hydrogenated at the edges to avoid unsaturated effects)

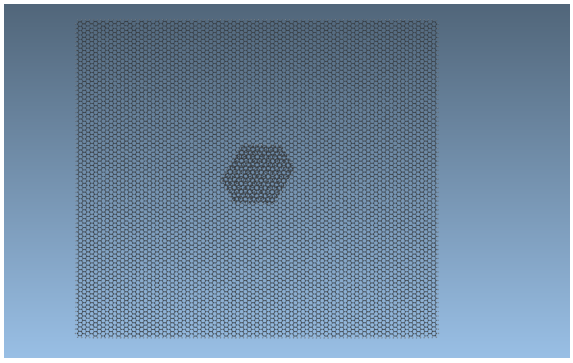

FIG. 4: 'Uncommensurate' (30° rotated from the stacked geometry) adsorption site studied for the 'large coronene' molecule on a large (20 nm per 20 nm) model graphene sheet (hydrogenated at the edges to avoid unsaturated effects)

The adsorption energy per carbon atom computed for the 'large coronene' molecule with ReaxFF is order 1.8 kcal/mol, *i.e.* 78 meV, per carbon atom (77.7 meV per carbon atom for the stacked configuration *vs.* 76.9 meV per carbon atom for the sandwich configuration), to be compared with 114 meV and 97 meV per carbon atom for the (stacked) adsorption energies of benzene and perylene respectively. Consequently, it seems that the total adsorption energy increases with the size of the adsorbed molecule, an expected additivity feature, but the mean adsorption energy per carbon atom decreases with increasing size of the latter. This trend is perfectly consistent with the results of Refs[13,14] of decreasing adsorption energy (in absolute value) per carbon atom with increasing number of carbon atoms – more precisely, with increasing ratio $\frac{N_C}{N_H}$ of hydrogen to carbon atoms numbers – in the polycyclic aromatic hydrocarbons. The adsorption energy between the molecule and the graphene sheet was indeed reported by Björk *et al.* to write as $N_C E_{CC} + N_H (E_{CH} - E_{CC})$ with E_{CC} and E_{CH} the adsorption energy per 'graphene-like' carbon (*i.e.* bonded to three other carbons) and 'benzene-like' carbon (*i.e.* bonded to two other carbons and one hydrogen) respectively.[13]

The stacked geometry is found again more stable than the sandwich geometry with ReaxFF force field : $E_{Stacked} < E_{Sandwich}$, with an energy difference :

$$\Delta E^{ReaxFF}_{Stacked/Sandwich} = -7.8 \text{ kcal/mol} \approx -339 \text{ meV} \quad (7)$$

which is in absolute value much larger than $k_B T \approx 25meV$ at $T = 300K$. Here, the adsorbed molecule is big enough so that the energy difference between the stacked and sandwich geometries found with ReaxFF are – despite being underestimated – much larger than the average thermal energy at room temperature. This indicates that under these temperature conditions the 'large coronene' stacked configuration has a much higher occurence probability with respect to its sandwich geometry counterpart, within ReaxFF model. Expressed per carbon atom, this difference of adsorption energies between the stacked and the sandwich configurations is of order 0.9 meV/C atom (378 carbon atoms in the 'large coronene' molecule).

The incommensurate geometry (obtained initially by rotating the stacked geometry of 'large coronene' by 30 degrees) minimization leads to a slightly more favorable adsorption than the sandwich geometry, but remains much less favorable than the stacked configuration, the differ-

Adsorption mode	Adsorption energy (ReaxFF)	Adsorption distance (ReaxFF)
Stacked	-675.8	3.26 $\AA$
Sandwich	-668.0	3.28 $\AA$
Rotated 30° (incommensurate)	-670.2	3.30 $\AA$

TABLE III: Comparison of adsorption energies of 'large coronene' (378 carbon atoms) on a very large (20 nm per 20 nm) hydrogenated graphene sheet. Minimizations are performed with ReaxFF as a force field. Energies are expressed in kcal/mol and distances in $\AA$.

ence being of the same order of magnitude :

$$\Delta E^{ReaxFF}_{Stacked/Rotated30^\circ} = -5.6 \text{ kcal/mol} \approx -244 \text{ meV} \quad (8)$$

which is also much larger than $k_BT \approx 25meV$ at room temperature. This is consistent with the literature on bilayer graphene sheets (see table V), where the most stable reported geometry for two graphene sheets is the ABAB stacked geometry [even relatively to incommensurate sheets of graphene, see below], which should be also the case here for a 'large coronene' molecule on top of a much larger graphene sheet.

Summary of the adsorption energies for stacked configurations :

We sum up the adsorption energies of the different molecules stacked (*i.e.* in the most favorable *AB* geometry) on top of a graphene sheet, and the energy barriers between the stacked *AB* configuration and the sandwich *AA* geometry found in this study (with ReaxFF force field) in Table IV. The trend obtained of decreasing binding energy (in absolute value) per carbon atom is consistent with Refs.,[13,14] as mentioned earlier. The equilibrium distances between the aromatic molecule and the underlying sheet do not seem to grow with molecule size, in contrast with what was reported in Ref.,[8] where they are respectively equal to 3.35 $\AA$ for benzene, 3.36 $\AA$ for naphtalene (two fused benzene cycles), 3.38 $\AA$ for a $C_{24}H_{12}$ coronene molecule and 3.40 $\AA$ for ovalene $C_{32}H_{14}$. This small discrepancy might be due to the different levels of theory used (ωB97X-D functional, STO-3G basis set in Ref.[8] *vs.* classical force field ReaxFF here) and to the much smaller size of the hydrogenated underlying graphene model ($C_{116}H_{28}$ used in Ref.[8] *vs.* $C_{873}H_{83}$ for benzene and perylene or $C_{13442}H_{330}$ for 'large coronene' here).

Comparison with results of the literature on graphene bilayers and on aromatic molecules adsorbed on a graphene sheet :

Our system made of a 'large coronene' molecule and a large graphene sheet mimicks locally a bilayer of two graphene sheets. It thus seems reasonable to compare the adsorption energies and distances, as well as the AB/AA energy separation, obtained with ReaxFF minimizations, with the corresponding results available in the literature for bilayer graphene.

In Ref.,[15] the *AB* stacked configuration is found the most stable whatever the relative angles between the two sheets and even whatever the curvature of the two graphene sheets (indicating that this stability result probably also holds for Double Walled carbon nanotubes). In this same article, an interlayer binding energy of -44 meV/atom was found for two flat graphene sheets in the stacked *AB* geometry ($\theta_i = \theta_0 = 0^\circ$, Fig. 2.(a), flat graphene sheets) and around -41 meV/atom for incommensurate sheets (rotation angle θ_i of one of the sheets with respect to the other below 10° and above 20°, avoiding the range near $\theta_0 = 16^\circ$) with a Kolmogorov-Crespi registry dependent interlayer interaction potential (of Lennard-Jones type). This yielded a difference in energy of 3 meV/atom between the stacked configuration and other rotated geometries (having at least 5° relative angle difference compared to the stacked case). Here, for 'large coronene', we found a difference in adsorption energy between the stacked *AB* geometry and the sandwich or rotated incommensurate geometry of about 0.9 meV/atom, which is slightly lower. This difference may be due to the fact that in Ref.[15] the two graphene sheets are relaxed (*i.e.* minimized) individually only, before the calculation of

Aromatic molecule	Benzene (C_6H_6)	Perylene ($C_{20}H_{12}$)	'Large coronene' ($C_{378}H_{48}$)
Number of C atoms	6	20	378
Adsorption energy (*AB* stacked geometry)	-16.25 kcal/mol (-707 meV)	-44.75 kcal/mol (-1.94 eV)	-675.8 kcal/mol (-29.4 eV)
Per atom (C and H) binding energy (*AB* geometry)	-1.35 kcal/mol (-59 meV)	-1.40 kcal/mol (-61 meV)	-1.59 kcal/mol (-69 meV)
Per carbon atom binding energy (*AB* geometry)	-2.7 kcal/mol (-114 meV)	-2.2 kcal/mol (-97 meV)	-1.79 kcal/mol (-78 meV)
Molecule-graphene distance (*AB* geometry)	3.22 $\AA$	3.27 $\AA$	3.26 $\AA$
AB-*AA* energy barrier $\Delta E_{AB/AA}^{ReaxFF}$	-0.15 kcal/mol (-6.5 meV) in total [1.1 meV / C atom]	-0.46 kcal/mol (-20 meV) in total [1.0 meV / C atom]	-7.8 kcal/mol (-339 meV) in total [0.9 meV / C atom]

TABLE IV: Comparison of adsorption energies and per-atom binding energies for the different polycyclic aromatic molecules studied on graphene. The most stable stacked *AB* configurations (on a much larger graphene sheet underneath) are chosen. Energies are derived from structural minimizations with ReaxFF as a force field.

the binding energy, instead of relaxing the whole system made of both sheets (as done here with ReaxFF for the graphene sheet and the above 'large coronene' molecule).

In Ref.,[16] the interaction energies between two graphene sheets was found to be -17.36 meV/atom and -17.72 meV/atom for the *AA* and *AB* stacking geometry respectively, using a simple Lennard-Jones potential and without considering energy stabilisation terms from π orbitals delocalisation in the *AB* configuration. These values were obtained for a particular set of Lennard-Jones parameters ($\varepsilon = 2.168$ meV and $\sigma = 3.36\AA$). Varying Lennard-Jones parameter sets made only the difference in energy between the *AA* and the *AB* geometry vary from -0.36 to -0.59 meV/atom, although the magnitude of the interaction energies of the two sheets in *AB* and *AA* configurations changed (-24.8 and -24.2 meV/atom for the *AB* and *AA* configuration respectively if $\varepsilon = 2.97$ meV and $\sigma = 3.4\AA$; -20.55 and -20.1 meV/atom for the *AB* and *AA* configuration if $\varepsilon = 2.5$ meV and $\sigma = 3.37\AA$, see Supplementary Material of Ref[16]).
This energy difference in the range -0.35 to -0.59 meV/atom is slightly lower but of the same order of -0.9 meV/atom found here for the difference between stacked *AB* and sandwich *AA* 'large coronene' – on a very large underlying graphene sheet. In Ref.[16] calculations were also done – as in Ref.[15] – with a fixed graphene sheet (made of 1560 atoms) and a movable graphene sheet of 336 atoms (edge effects were neglected). The interlayer energy for turbostratic structures (*i.e.* two parallel rotated sheets) were also studied, estimating the energy difference per atom between the *AB* stacking and incommensurate configurations to be $-17.72 + 17.61 = -0.11$ meV/atom in average.

In Ref.,[17] DFT calculations at the LDA level (periodized system, and without a vdW correction term) yielded a magnitude of -20 meV/atom interlayer energy for *AB* stacking, and a difference of interlayer energy of 9.7 meV/atom between *ABAB* Bernal graphite and *AAAA* stacking (with a unit cell and periodic boundary conditions necessary for the expansion in plane waves basis sets), much larger than the energy barrier estimated here with ReaxFF. These results being calculated for bulk graphite (unit cell spanning 3 neighboring layers, with periodic boundary conditions), made of an infinite number of graphene sheets, the cohesive energy per atom includes implicitly the interaction with the two neighboring sheets (one being above, the other one being below). Thus, to convert it in terms of cohesive energy per atom for a system of two neighboring sheets only, these energies have to be divided by two (assuming that only nearest neighbor layers interact with each other, *i.e.* neglecting interactions between non contiguous layers). The very small magnitude of the interlayer energy of -10 meV/atom obtained thereby is consistent with the fact that Charlier *et al.* did not use dispersion correction terms to the DFT electronic energy in Ref.,[17] but rather assumed that dispersion interactions were hidden in the exchange-correlation term.

A recent study of quantum Monte-Carlo calculations of the binding energy of bilayer graphene compared the existing values in the literature of graphene bilayer binding energies derived with DFT methods, with or without dispersion correction.[18] It appears that there is little consensus on the magnitude of the binding energy

System	Interlayer binding energy	Equilibrium distance	Method used	Number of atoms	Energy difference between *AB* and *AA* configurations $\Delta E_{AB/AA}$	Reference
Two-circular shaped graphene sheets (diameter 16 nm)	-44 meV/atom	3.34 Å	Kolmogorov-Crespi registry-dependent interlayer interaction potential (modified LJ)	15 355 atoms (two sheets)	-3 meV/atom	15
Two flat graphene sheets (one fixed, one movable)	-17.72 meV/atom (*AB* stacking) *vs.* -17.36 meV/atom (*AA* stacking)	3.35 Å (*AB* stacking) and 3.38 Å (*AA* stacking)	Lennard-Jones potential $4\varepsilon\left[\left(\frac{\sigma}{r}\right)^{12}-\left(\frac{\sigma}{r}\right)^{6}\right]$ ($\varepsilon = 2.168meV$ and $\sigma = 3.36$Å)	1560 atoms (sheet underneath) and 366 atoms (movable sheet)	From -0.59 to -0.36 meV/atom	16
Graphene bilayer	−17.7 meV/atom (*AB* stacking) *vs.* −11.5 meV/atom (*AA* stacking)	3.43 Å	Diffusion quantum Monte-Carlo calculations	3 × 3 supercell, PBC$^{(*)}$	-6.2 meV/atom	18
ABAB graphite and *AAAA* stacking of sheets	-20 meV/atom in graphite (-11.6 meV/atom due to E_{xc}) *i.e.* -10 meV/atom for two sheets only	3.30 Å (*AB* stacking) and 3.66 Å (*AA* stacking)	DFT (LDA functional, vdW dispersion assumed included in the exchange-correlation term E_{xc}), plane waves basis set (cutoff energy 1360 eV).	Unit cell (4 atoms for *AB* stacking), PBC$^{(*)}$	-9.7 meV/atom for graphite *i.e.* -4.9 meV/atom for two sheets	17
Graphene bilayer	-50.6 meV/atom (DFT-D), -29.3 meV/atom (vdW-DFT)	3.25 Å	DFT-D (PBE functional and semi-empirical corrections for dispersion terms,[22] plane-wave basis (cutoff energy 400 eV) using Projector Augmented Wave method), and vdW-DFT[23] (same DFT conditions, non-local dispersion corrections)	4.271 Å× 2.466 Å× 20 Å cell, PBC$^{(*)}$	-19.5 meV/atom (DFT-D), -18.9 meV/atom (vdW-DFT)	20
Graphene bilayer ('AB' stacking geometry)	-48 meV/atom (-51 meV/atom for a graphene trilayer)	3.45 Å	vdW-DFT[23] (dispersion corrections through a non-local density functional). Double zeta polarized basis sets of pseudo atomic orbitals.	Unit cell : 18.7 Å × 20.7 Å in the *x*, *y* directions, 20 Å in the vertical direction, PBC$^{(*)}$	Not studied	14

TABLE V: Interlayer binding energies found in the literature for graphene bilayers systems. Energies are expressed in meV per carbon atom (1 kcal/mol = 43 meV), distances in Å . $(*)$ PBC refers to Periodic Boundary Conditions.

for bilayer graphene, as values range from −70 to −10.4 meV/atom. However, most authors seem to agree that *AB* stacking is the most stable and that *AA* the least, except Ref.[19] reporting that *AA* stacking is the most stable at the (semi-empirical) PM6-DH2 level – including corrections both for dispersion and H-bonding interactions – for benzene on a graphene model made of 1006 atoms. In Ref.,[18] the authors found −17.7 meV/atom binding energy for bilayer graphene in *AB* stacking, *vs.* −11.5 meV/atom in *AA* stacking, using diffusion quantum Monte Carlo.

The spread of the values of graphene bilayer binding energies observed in the literature is related to the difficulty to model accurately $\pi-\pi$ stacking weak interactions – which drive the adsorption of conjugated polyfluorenes on CNT surfaces, for instance. In DFT, the variety of choices for pseudo-potentials, basis sets and exchange-correlation functionals is mostly accountable for the large dispersion in these results. Dispersion interactions are reported as the main contributor to the binding of graphene bilayers or polyaromatic cycle molecules on graphene.[4,8,20,21] Correction terms – *e.g.* semi-empirical as proposed by Grimme[10] and reviewed in Ref.[12] – to account for these dispersion interactions (quantum fluctuation effects, one component of the three types of van der Waals interactions) within DFT are thus mandatory. They should yield a lower variability across different studies – given their simple analytical expression – than the electronic energy counterpart (in DFT). Yet some deviations are also observed in the literature for the magnitude of the contribution of dispersion correcting terms to the AB/AA energy barrier (in DFT-D studies), as will be discussed in the conclusion below. All the results discussed in this section reported in the literature on bilayer graphene are summarized in Table V. The literature results for aromatic molecules on a graphene sheet are also summed up in Table VI.

System	Binding energy	Equilibrium distance	Method used	Number of atoms	Energy difference between AB and AA configurations $\Delta E_{AB/AA}$	Reference
Benzene on graphene	-40 meV/C atom (-240 meV in total)	3.17 $\AA$ (AB stacking) and 3.40 $\AA$ (AA stacking)	DFT (LDA exchange-correlation functional, plane-wave basis with 240 eV cutoff energy), no vdW correction.	6 C atoms (benzene), 12.3 $\AA$ × 12.3 $\AA$ × 10 $\AA$ graphene supercell (50 C atoms), PBC$^{(*)}$	-13.3 meV/C atom (-80 meV in total)	24
Benzene on CNT	≈ -30 meV/C atom (≈ -190 meV in total)	3.20 to 3.27 $\AA$, "bridge" configuration the most stable (over a C-C bond)	DFT (LDA exchange-correlation), no vdW correction, localized pseudoatomic orbitals (split-valence double-ζ basis set, including polarization and extended 3s orbitals for C and double-ζ for H), BSSE corrected.	6 C atoms (benzene) and CNT, supercell and PBC$^{(*)}$.	$\Delta E_{AB/AA}$ not studied. $\Delta E_{bridge/stacked} \approx -15meV$ *i.e.* ≈ -2 meV/C atom	2
Benzene on a graphene model (C_{574} to C_{1006})	-96 to -76 meV/C atom (-574 to -457 meV in total)	Not precised	Dispersion corrected semi-empirical method (MO theory) PM6-DH2, compared to DFT (B3LYP-D, M06-2X and ωB97X-D functionals), several basis sets tested (*e.g.* 6-311G(2d,2p) and TZV2D with ωB97X-D)	6 C atoms (benzene) and graphene model (medium-size finite sheet). Solvent (H_2O) also considered.	Not studied (averages over configurations close in energy were done)	19
Benzene on a hydrogenated graphene model (C_{1006})	-83 meV/C atom (-496 meV in total)	3.29 $\AA$	PM6-DH2 (single point calculation, geometry optimized at OPLS-AA level). Results in agreement with ωB97X-D/cc-pVDZ level (BSSE corrected).	6 C atoms (benzene) and 1006 C atoms in the graphene model.	Not studied.	25
Benzene stacked on a $C_{150}H_{30}$ coronene (graphene model)	-87 meV/C atom (-522 meV in total)	Not precised	Symmetry adapted perturbation theory (SAPT)	6 C atoms (benzene)	Not studied	21
Benzene stacked on $C_{110}H_{26}$ ('coronene 43') graphene model	-92 meV/C atom (-552 meV in total)	'AB' (3.35 $\AA$) and 'PD' (3.34 $\AA$) optimized adsorption geometries ('PD' slightly more stable)	ωB97X-D/def2-TZVPP level, (DFT, semi-empirical vdW correction,[9] TZVPP basis sets)	6 C atoms (benzene)	$\Delta E_{AB/AA} \approx$ -6.3 meV/C atom, $\Delta E_{PD/AB} \approx$ -0.15 meV/C atom	26 (same authors as Ref.[21])
Benzene stacked on $C_{110}H_{26}$ ('coronene 43') graphene model	-99 meV/C atom (-595 meV in total)	'AB' (3.35 $\AA$) and 'PD' (3.34 $\AA$) optimized adsorption geometries	(Spin Component Scaled) SAPT0, aug-cc-pVDZ basis set	6 C atoms (benzene)	$\Delta E_{PD/AB} \approx$ -0.2 meV/C atom	26 (same authors as Ref.[21])
Benzene on graphene (periodized)	-136 meV/C atom	3.22 $\AA$ (AB stacking), 3.26 $\AA$ (AA stacking)	DFT-D (PBE exchange-correlation functional (GGA type), semi-empirical dispersion corrections,[6] plane wave basis sets (cutoff energy 415 eV), Projector Augmented Wave method)	6 C atoms (benzene), p(4×4) supercell of the graphene sheet (PBC$^{(*)}$)	-8.5 meV/ C atom, -5.9 meV/C atom due to $\Delta E^{vdW}_{AB/AA}$ and -2.6 meV/ C atom due to $\Delta E^{DFT}_{AB/AA}$.	4
Benzene on a (hydrogenated) graphene model ($C_{116}H_{28}$)	-78.3 meV/C atom (-470 meV total binding energy)	3.35 $\AA$	ωB97X-D (DFT level, semi-empirical vdW correction), 6-31G* basis-set	6 C atoms (benzene)	-9.4 meV/C atom (-5.1 meV/ C atom with STO-3G basis)	8
Coronene ($C_{24}H_{12}$) on graphene model ($C_{116}H_{28}$)	-72 meV/C atom (-1.73 eV total binding energy)	3.38 $\AA$	ωB97X-D (DFT level, semi-empirical vdW correction), 6-31G* basis-set	24 C atoms (coronene)	-11 meV/ C atom (-5.1 meV/ C atom with STO-3G basis)	8

TABLE VI: Interlayer binding energies or adsorption energies found in the literature for aromatic molecules adsorbed on a graphene sheet. Energies are expressed in meV per carbon atom, distances in $\AA$. $(*)$ Periodic Boundary Conditions.

The influence of edge-effects in finite systems (aromatic molecules on a graphene sheet as opposed to two infinite interacting graphene layers) has been studied in.[8] It is certainly necessary to be cautious when comparing adsorption energies on graphene of small aromatic molecules like benzene with the interlayer energies of two graphene sheets. For instance, in Ref.,[8] the value of -11 meV per carbon atom found as energy barrier $\Delta E_{AB/AA}$ for a coronene $C_{24}H_{12}$ molecule on a graphene model is extrapolated to be the energy difference (barrier) per atom between stacked AB and hollow AA configurations in an infinite graphene bilayer (see Table

System	Binding energy	Equilibrium distance	Method used	Number of atoms	Energy difference between AB and AA configurations $\Delta E_{AB/AA}$	Reference
Benzene on (hydrogenated) graphene model ($C_{873}H_{83}$)	-114 meV/C atom	3.22 $\AA$	ReaxFF (parametrization[1])	6 C atoms (benzene)	-1.1 meV/C atom	This work
Perylene on (hydrogenated) graphene model ($C_{873}H_{83}$)	-97 meV/C atom	3.27 $\AA$	ReaxFF (parametrization[1])	20 C atoms (perylene)	-1.0 meV/C atom	This work
'Large coronene' on (hydrogenated) graphene model ($C_{13442}H_{330}$)	-78 meV/C atom	3.22 $\AA$	ReaxFF (parametrization[1])	378 C atoms ('large coronene'), (20 nm $\times$ 20 nm) graphene monolayer	-0.9 meV/C atom	This work

TABLE VII: Adsorption energies found with ReaxFF structural minimizations for aromatic molecules adsorbed on a graphene sheet. Energies are expressed in meV per carbon atom, distances in $\AA$.

VI).

D. Conclusion on the use of ReaxFF as a force field for CNT/ conjugated polymer compounds interaction studies

The magnitude of the interlayer binding energy is satisfactorily reproduced by ReaxFF (both compared to experimental or higher level of theory values), although there is some deviation in the values reported in the literature, derived from different levels of theories in DFT (due to different choices of pseudo-potentials, exchange-correlation functionals, basis sets, or dispersion correction methods, among others). Although ReaxFF captures the relative stability of AB stacking compared to AA stacking, the separation in energy between these two extreme configurations is much lower than what is obtained in average with DFT-D (see Tables VI and VII for comparison). It is expected that DFT-D level of theory better captures this separation in energy as it is mainly due to the overlap of electronic clouds of the two adjacent layers,[17] which is strongly anisotropic and highly dependent on the in-plane relative displacement between the two sheets. However, no experimental value for the AB/AA energy barrier is available.

The separation in energy $\Delta E_{AB/AA}$ obtained with ReaxFF is similar to the results of methods based on Lennard-Jones potential only, as seen from Table V. Lennard-Jones potential is known to strongly underestimate the barrier $\Delta E_{AB/AA}$ (see Ref.[20] and discussion on the corrugation of the potential relief *i.e.* the barrier height in the bilayer graphene translational energy landscape). In fact, the underestimation of the actual energy barrier is more due to overlooking other terms (as energy stabilization terms from overlapping of neighboring electron clouds of the two sheets) than to the bad performance of Lennard-Jones model itself. Indeed, dispersion interactions, represented by Lennard-Jones potential, have been reported not to play a significant role on the values of the barrier $\Delta E_{AB/AA}$, and more generally on the barrier in the relative motion of polyaromatic hydrocarbons (PAHs) on hydrogen-terminated graphene.[8]

In other words, Lennard-Jones interactions are the main contributor to the whole $\pi-\pi$ stacking interactions – that is why binding energy calculations based on Lennard-Jones potential, only, yield the good order of magnitude of interlayer binding energies (-44 meV/atom in[15] which is in the experimental range) – but do not vary much with respect to the stacking configurations (AB, AA, or rotated/incommensurate). Thus Lennard-Jones interaction terms alone cannot be held accountable for the AB/AA energy separation, which they cannot reproduce with the good order of magnitude. Hence the energy difference found between AB and AA configurations is about 0.3 to 0.6 meV/atom (in absolute value) only with a Lennard-Jones potential,[15] while energy differences $\Delta E_{AB/AA}$ in the range 6 to 20 meV/atom (in absolute value) were reported in DFT calculations[17,18,20] when the electronic energy, computed from the density, is included. Energy barriers computed with MM3 and MM4 force fields (that include a Lennard-Jones like potential term to account for vdW interactions) reported an energy barrier $\Delta E_{AB/AA} \approx 0.5$ meV/atom[20] in the same range, once again one order of magnitude smaller than the energy barriers found with DFT. This is consistent with the results concerning the influence of dispersion interactions reported in Ref.[8] Lebedeva *et al.* also report that the energy barrier

$\Delta E_{AB/AA}$ calculated with Lennard-Jones potential is underestimated by an order of magnitude with respect to DFT-D calculations[20] (because van der Waals dispersion interactions are only accountable for around 10 % of the energy separation between *AB* and *AA* geometries).

To sum it up simply, although van der Waals dispersion interactions are the main contributor to the energy in layered systems or non-covalently interacting aromatic compounds, they cannot account qualitatively for energy differences between different stacking geometries in the case of graphene bilayers, or aromatic molecules adsorbed parallel to a graphene sheet. These energy differences seem overwhelmingly due to electronic orbitals and hybridization effects and can be computed *e.g.* through DFT.

The previous analysis is somewhat tempered by the results obtained by Kozlov and al. in Ref.[4] (to which we previously compared ReaxFF for six adsorption modes of benzene on graphene) where diffusion energy profiles calculations with DFT-D methods were done, to study the energy barriers that a benzene or a polycyclic aromatic molecule has to overcome when diffusing rigidly, parallel to a graphene sheet, changing continously of adsorption site. These results yield in particular the following decomposition of the energy difference between stacked and sandwich configurations for benzene :

$$\Delta E^{tot}_{AB/AA} = \Delta E^{vdW}_{AB/AA} + \Delta E^{DFT}_{AB/AA} \approx -5.9 \text{ meV/C atom} - 2.6 \text{ meV/C atom} = -8.5 \text{ meV/C atom} \quad (9)$$

i.e. the energy difference accounted by the semi-empirical dispersion corrections to the DFT energy, namely $\Delta E^{vdW}_{AB/AA} \approx -5.9$ meV/C atom, between these two extreme adsorption sites, is the main contributor to $\Delta E^{tot}_{AB/AA}$. The results of Ref.[4] are in contradiction, among others, with the results described above from Ershova and al.[8] and Lebedeva et al.[20] who showed that the difference of vdW dispersion interactions energies between *AB* and *AA* geometries is lower by one order of magnitude than the pure DFT energy component (*i.e.* should not account for more than 10 % of this energy difference).

Finally, ReaxFF captures the good order of magnitude of $\pi-\pi$ stacking binding energies but does not separate *AB* and *AA* configurations as correctly as DFT-D does, as expected. As seen in Table VII, ReaxFF (with this particular parametrization) performs better than Lennard-Jones potential to separate these *AB* and *AA* geometries, but slightly worse than Kolmogorov-Crespi type potentials,[15] which in turn separates much less *AB* and *AA* geometries than DFT-D methods (*e.g.* ω-B97X-D/6-31G*) as in Ref.[8,17,18,20]

In conclusion, ReaxFF should be deemed a reasonable force field to simulate large systems where $\pi-\pi$ stacking interactions are very significant – as for CNT/conjugated polymer hybrids – and discuss the main geometrical features (does adsorption occur, are monomer units parallel or perpendicular to the surface, is the polymer chain coiled or perfectly adsorbed on the surface, etc.). However, it cannot be used to conclude on the details of the relative orientation of the polymer chain with respect to the CNT surface – *e.g.* to know the angles between the polymer backbone and the carbon hexagonal lattice underneath – given that the energy barrier for translation of aromatic compounds along the surface is too low.

[1] Alejandro Strachan, Adri C. T. van Duin, Debashis Chakraborty, Siddharth Dasgupta, and William A. Goddard. Shock waves in high-energy materials: The initial chemical events in nitramine RDX. *Physical Review Letters*, 91(9), aug 2003.

[2] F. Tournus and J.-C. Charlier. Ab initiostudy of benzene adsorption on carbon nanotubes. *Physical Review B*, 71(16), apr 2005.

[3] F. Tournus, S. Latil, M. I. Heggie, and J.-C. Charlier. π-stacking interaction between carbon nanotubes and organic molecules. *Physical Review B*, 72(7), aug 2005.

[4] Sergey M. Kozlov, Francesc Viñes, and Andreas Görling. On the interaction of polycyclic aromatic compounds with graphene. *Carbon*, 50(7):2482–2492, jun 2012.

[5] Henna Ruuska and Tapani A. Pakkanen. Ab initio study of interlayer interaction of graphite: benzene-coronene and coronene dimer two-layer models. *The Journal of Physical Chemistry B*, 105(39):9541–9547, oct 2001.

[6] F. Ortmann, F. Bechstedt, and W. G. Schmidt. Semiempirical van der waals correction to the density functional description of solids and molecular structures. *Physical Review B*, 73(20), may 2006.

[7] Renju Zacharia, Hendrik Ulbricht, and Tobias Hertel. Interlayer cohesive energy of graphite from thermal desorption of polyaromatic hydrocarbons. *Physical Review B*, 69(15), apr 2004.

[8] Olga V. Ershova, Timothy C. Lillestolen, and Elena Bichoutskaia. Study of polycyclic aromatic hydrocarbons adsorbed on graphene using density functional theory with empirical dispersion correction. *Physical Chemistry Chemical Physics*, 12(24):6483, 2010.

[9] Jeng-Da Chai and Martin Head-Gordon. Long-range corrected hybrid density functionals with damped atom–atom dispersion corrections. *Physical Chemistry Chemical Physics*, 10(44):6615, 2008.

[10] Stefan Grimme. Semiempirical GGA-type density functional constructed with a long-range dispersion correction. *Journal of Computational Chemistry*, 27(15):1787–1799, 2006.

[11] Petr Jurečka, Jiří Šponer, Jiří Černý, and Pavel Hobza. Benchmark database of accurate (MP2 and CCSD(T) complete basis set limit) interaction energies of small model complexes, DNA base pairs, and amino acid pairs. *Phys. Chem. Chem. Phys.*, 8(17):1985–1993, 2006.

[12] Stefan Grimme. Density functional theory with london dispersion corrections. *Wiley Interdisciplinary Reviews: Computational Molecular Science*, 1(2):211–228, mar 2011.

[13] Jonas Björk, Felix Hanke, Carlos-Andres Palma, Paolo Samori,

Marco Cecchini, and Mats Persson. Adsorption of aromatic and anti-aromatic systems on graphene through π-π stacking. *The Journal of Physical Chemistry Letters*, 1(23):3407–3412, nov 2010.

[14] Steven Bailey, David Visontai, Colin J. Lambert, Martin R. Bryce, Harry Frampton, and David Chappell. A study of planar anchor groups for graphene-based single-molecule electronics. *The Journal of Chemical Physics*, 140(5):054708, feb 2014.

[15] Yufeng Guo and Wanlin Guo. Interlayer energy-optimum stacking registry for two curved graphene sheets of nanometre dimensions. *Molecular Simulation*, 34(8):813–819, jul 2008.

[16] Yasushi Shibuta and James A. Elliott. Interaction between two graphene sheets with a turbostratic orientational relationship. *Chemical Physics Letters*, 512(4-6):146–150, aug 2011.

[17] J.-C Charlier, X Gonze, and J.-P Michenaud. Graphite interplanar bonding: Electronic delocalization and van der waals interaction. *Europhysics Letters (EPL)*, 28(6):403–408, nov 1994.

[18] E. Mostaani, N. D. Drummond, and V. I. Fal'ko. Quantum monte carlo calculation of the binding energy of bilayer graphene. *Physical Review Letters*, 115(11), sep 2015.

[19] Mark A. Vincent and Ian H. Hillier. Accurate prediction of adsorption energies on graphene, using a dispersion-corrected semiempirical method including solvation. *Journal of Chemical Information and Modeling*, 54(8):2255–2260, aug 2014.

[20] Irina V. Lebedeva, Andrey A. Knizhnik, Andrey M. Popov, Yurii E. Lozovik, and Boris V. Potapkin. Interlayer interaction and relative vibrations of bilayer graphene. *Physical Chemistry Chemical Physics*, 13(13):5687, 2011.

[21] Weizhou Wang, Tao Sun, Yu Zhang, and Yi-Bo Wang. Substituent effects in the $\pi - \pi$ interaction between graphene and benzene: An indication for the noncovalent functionalization of graphene. *Computational and Theoretical Chemistry*, 1046:64–69, oct 2014.

[22] Vincenzo Barone, Maurizio Casarin, Daniel Forrer, Michele Pavone, Mauro Sambi, and Andrea Vittadini. Role and effective treatment of dispersive forces in materials: Polyethylene and graphite crystals as test cases. *Journal of Computational Chemistry*, 30(6):934–939, apr 2009.

[23] M. Dion, H. Rydberg, E. Schröder, D. C. Langreth, and B. I. Lundqvist. Van der waals density functional for general geometries. *Physical Review Letters*, 92(24), jun 2004.

[24] Yong-Hui Zhang, Kai-Ge Zhou, Ke-Feng Xie, Jing Zeng, Hao-Li Zhang, and Yong Peng. Tuning the electronic structure and transport properties of graphene by noncovalent functionalization: effects of organic donor, acceptor and metal atoms. *Nanotechnology*, 21(6):065201, jan 2010.

[25] Evgeniy G. Gordeev, Mikhail V. Polynski, and Valentine P. Ananikov. Fast and accurate computational modeling of adsorption on graphene: a dispersion interaction challenge. *Physical Chemistry Chemical Physics*, 15(43):18815, 2013.

[26] Weizhou Wang, Yu Zhang, and Yi-Bo Wang. Noncovalent $\pi - \pi$ interaction between graphene and aromatic molecule: Structure, energy, and nature. *The Journal of Chemical Physics*, 140(9):094302, mar 2014.